A SIMPLE METHOD FOR TIMING AN XFEL SOURCE TO HIGH-POWER LASERS

G. Geloni, E. Saldin, E. Schneidmiller, M. Yurkov
DESY/XFEL, Notkestrasse 85, 22607 Hamburg, Germany

Abstract

We propose a technique for timing an XFEL to a high-power laser with femtosecond accuracy. The same electron bunch is used to produce an XFEL pulse and an ultrashort optical pulse that are, thus, naturally synchronized. Cross-correlation techniques will yield the relative jitter between the optical pulse (and, thus, the XFEL pulse) and a pulse from an external pump-laser with femtosecond resolution. Technical realization will be based on an optical replica synthesizer (ORS) setup to be installed after the final bunch-compressor. The electron bunch is modulated in the ORS by an external optical laser. Travelling through the main undulator, it produces the XFEL pulse. Then, a powerful optical pulse of coherent edge radiation is generated as the bunch passes through a long straight section and a separation magnet downstream of the main undulator. Relative synchronization of these pulses is preserved using the same mechanical support for X-ray and optical elements transporting radiation to the experimental area, where single-shot cross-correlation between optical pulse and pump-laser pulse is performed. We illustrate our technique with numerical examples referring to the European XFEL. **For a more extensive treatment and references we redirect the reader to [1].**

TIMING SYSTEM DESCRIPTION

With the realization of x-ray free electron lasers (XFELs), pump-probe experiments will be used to monitor time-dependent phenomena with femtosecond accuracy and atomic resolution. Relative synchronization of radiation pulses from XFEL and optical laser on the femtosecond level can be relaxed when information on the temporal jitter between XFEL pulse and pump-laser pulse is kwown. In fact, if the time shift between pump and probe pulse can be measured on-line with femtosecond time-resolution, jitter can be used to randomly sample various time-delays in the pump-probe experiment, which are subsequently sorted up. Based on this observation, we propose a concept of time-arrival monitor allowing measurement of relative delay between FEL and optical pulses on a fs time scale.

Elements of the system are an optical modulator and an optical radiator (see Fig. 1).

Operation of the optical modulator

A laser pulse is used to modulate the electron energy at the same wavelength by interaction in a short modulator-undulator. Subsequently, the electron bunch passes through a dispersion section, where the energy modulation induces a density modulation at the seed-laser wavelength λ. The amplitude of density modulation at the exit of the chicane approaches $a_i = R_{56}(\Delta\gamma)_i/(\lambda\!\!\!^{-}\gamma_0)\exp\left[-\left\langle(\delta\gamma)^2\right\rangle R_{56}^2/(2\gamma_0^2\lambda\!\!\!^{-2})\right]$, so that the current is $I = I_0[1 + a_i\cos(\psi)]$. Here $\psi = \omega[z/v_z(\gamma_0) - t]$ is the modulation phase (v_z is the longitudinal velocity of a nominal electron, $\omega = 2\pi c/\lambda$, c is the speed of light in vacuum, t is the time), and I_0 is the unmodulated electron beam current. Moreover, R_{56} is the compaction factor of the dispersion section, $(\Delta\gamma)_i\sin(\psi)$ and $\left\langle(\delta\gamma)^2\right\rangle^{1/2}$ are the energy modulation and the rms uncorrelated energy spread of the electron bunch in units of the rest mass. Finally, $\lambda\!\!\!^{-} = \lambda/(2\pi)$ is the reduced modulation wavelength. The modulator to be used is the already foreseen optical replica modulator. In the case of the European XFEL (see Fig. 2) $\gamma_0 \simeq 4\cdot 10^3$, (2 GeV), $\left\langle(\delta\gamma)^2\right\rangle^{1/2} \simeq 2$ (1 MeV rms uncorrelated energy spread), $(\Delta\gamma)_i \simeq 1$, (0.5 MeV modulation), and $\lambda = 400$ nm (second harmonic of a Ti:Si laser). A value $R_{56} \simeq 30\mu$m leads to a modulation amplitude $a_i \simeq 0.1$.

The density modulation reaches an amplitude of about 10%. Following the dispersion section the bunch goes through the main linac and the collimator. Finally, it enters the x-ray undulator. Since a high-current (about 5 kA) electron beam is transported, the initial density modulation produces an energy modulation due to longitudinal impedance caused by space-charge fields through the linac. Energy and density modulation can be shown to obey [1]

$$\frac{da}{dz} = \frac{1}{\lambda\!\!\!^{-}}\frac{\Delta\gamma(z)}{\gamma^3(z)}\,,$$
$$\frac{d(\Delta\gamma)}{dz} \simeq -\frac{a(z)}{\lambda\!\!\!^{-}\gamma^2(z)}\frac{I_0}{I_A}\exp\left[\frac{\epsilon_n\beta}{\gamma^3(z)\lambda\!\!\!^{-2}}\right]\Gamma\left[0,\frac{\epsilon_n\beta}{\gamma^3(z)\lambda\!\!\!^{-2}}\right] \quad (1)$$

Here Γ is the incomplete gamma function, β is the average betatron function in the accelerator, and ϵ_n is the normalized emittance.

We assume $\beta = 25$ m along the main accelerator and $\epsilon_n = 1.4$ mm·mrad. Setting the acceleration length $d_a \simeq 1220$ m (see Fig. 2) and $I_0 \simeq 5$ kA, numerical analysis of Eq. (1) shows that our initial conditions $a_i \simeq 0.05$ and $(\Delta\gamma)_i \simeq 1$ yield, at the entrance of the collimator, $z = d_c$, $a(d_c) \simeq 0.03$ and $\Delta\gamma(d_c) \simeq -6$.

The nominal value of the compaction factor of the collimator $R_{56}^{(c)}$ is set to zero[1], with possibility of fine tuning around this value of about ± 100 μm. Thus we set

[1]Pending design finalization, $R_{56}^{(c)}$ maybe chosen within ±1 mm. For any choice, initial conditions can be set to obtain acceptable a_f and $(\Delta\gamma)_f$.

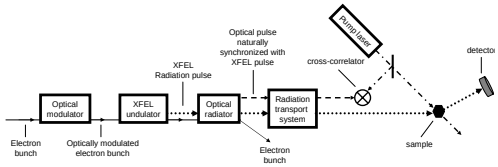

Figure 1: Timing scheme at an XFEL setup.

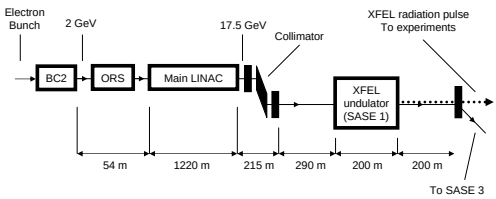

Figure 2: Proposed monitor at the European XFEL.

$R_{56}^{(c)} \simeq +50\mu$m, at the exit of the collimator to obtain $a_c \simeq -0.1$, whereas $(\Delta\gamma)_c \simeq -6$.

Further on, energy and density modulation should be propagated through a straight section followed by the main XFEL undulator. We can use the same set of equations (1), setting $g = 0$, using an energy of 17.5 GeV and an average value of the betatron function $\beta = 20$m. At the entrance of the XFEL undulator one has $a(d_u) \simeq -0.1$, while $\Delta\gamma(d_u) \simeq -5$. Numerical analysis with the code FAST shows that such an energy modulation, being smaller than the foreseen XFEL spectral bandwidth 0.08%, will not alter the XFEL process (see Figs. 3 and 4, where amplitude and period of electron bunch modulation are 10% and 400 nm respectively, and results are calculated for SASE 1 at the European XFEL).

Similarly as before, the passage in the main XFEL undulator has the effect of decreasing the energy modulation level. Moreover, although the undulator is shorter than the straight section preceding it, the effect on the energy modulation is stronger. In fact, the longitudinal Lorentz factor inside the undulator is $\gamma_z = \gamma/\sqrt{1+K^2}$. Since $K = 3.3$, γ^2 and γ_z^2 differ of about an order of magnitude, hence a different influence of the undulator compared with the straight section. It turns our from numerical analysis with previously found initial conditions $a(d_u)$ and $\Delta\gamma(d_u)$, and using $\beta = 40$m, that the energy and density modulation levels at the radiator entrance, $a_f \simeq -0.1$ and $(\Delta\gamma)_f \simeq -2$.

It follows that the optical modulator can induce about 10% density modulation at the entrance of the optical radiator, $|a_f| \simeq 0.1$, and acceptable energy modulation, independently of the design of the collimation section, without perturbation of the FEL process in the baseline undulator.

Operation of the optical radiator

The bunch resulting from the modulator can be considered as a filament, as it is modulated in density at a wavelength much longer than the geometrical emittance

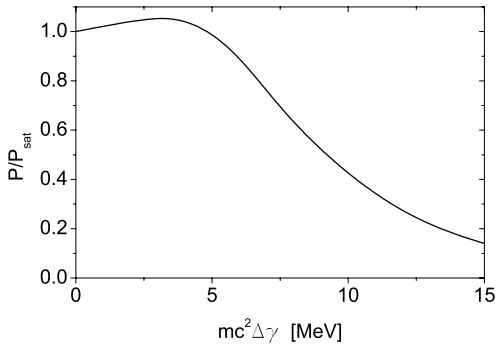

Figure 3: Output power vs. energy modulation. Radiation power is normalized to saturation power at $\Delta\gamma = 0$.

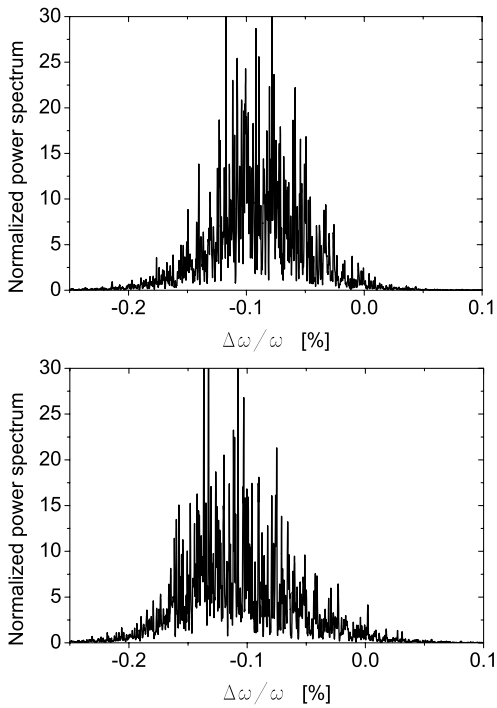

Figure 4: Normalized spectrum at zero energy modulation (upper plot), and at $\Delta\gamma mc^2 = 4$ Mev (lower plot).

of the beam. The transverse components of the Fourier transform of the electric field form a vector $\vec{E}(\vec{r}, z)$, dependent on transverse and longitudinal coordinates $\vec{r}$ and z. From the paraxial approximation follows that the envelope $\tilde{\vec{E}} = \vec{E}\exp[-iz/\lambda\!\!\!^{-}]$, does not vary much along z on the scale of the reduced wavelength $\lambda\!\!\!^{-}$. With some abuse of language we will call $\tilde{\vec{E}}$ "the field". The field obeys the paraxial wave equation in the space-frequency domain, where the source-term vector is specified by the trajectory of the source electrons, and can be written in terms of the Fourier transform of the transverse current density, $\vec{j}(z, \vec{r}, \omega)$, and of the charge density, $\bar{\rho}(z, \vec{r}, \omega)$, which are regarded as given data. In this paper we will treat them as macroscopic quantities, without investigating individual electron contributions.

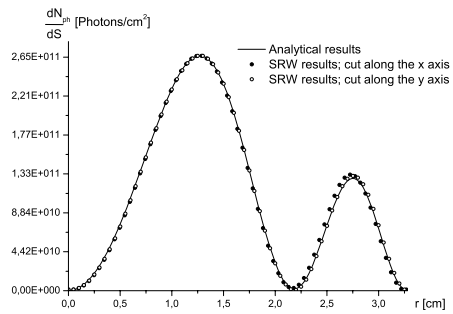

Figure 5: Photon density distribution vs. radial position at the first optical element, $z = 400$ m.

As concerns emission of coherent optical radiation, our setup reduces to an upstream bending magnet (the last bend of the collimator), a straight section, an undulator (the main SASE 1 undulator), a second straight section and a downstream separation bending magnet (see Fig. 2). A photon stop will be installed inside the main undulator, whose main function is that of absorbing spontaneous radiation background. Moreover, an extra photon stop might be installed at the exit of the main undulator, absorbing all but the SASE pulse. As a result, for estimations of the effect, one has to deal with the simple situation where the optical radiator is composed by a single straight section between the exit of the undulator and the separation magnet.

When a modulated beam passes through a straight section of length L limited by upstream and downstream bending magnets of radius R, it produces edge radiation. By comparing the radiation formation length of the bending magnet field with that of the straight section, one can show that the influence of bending magnet radiation to the field contribution is negligible with an accuracy 10^{-3}, and a sharp-edge approximation applies.

Then, the system radiates in the same way as two virtual sources located at the edges of the straight section [1]. These sources can be described analytically in a simple way. Choosing the origin of the longitudinal axis in the center of the downstream straight section and letting $L \equiv L_2$ we can characterize the two virtual sources through $\vec{\vec{E}}(\pm L/2, \vec{r}) = \mp 2ie/(c\gamma\lambda)\exp\left[\pm iL/(4\gamma^2\lambda)\right]\vec{r}/r \cdot K_1\left[r/(\gamma\lambda)\right]$. Propagation from the sources to any distance z down the beamline can be performed, and the radiation energy density can be calculated as $dW/(d\omega dS) = e^2/(4\pi^2\lambda Lc)F(z,\vec{r})$, with $F(z,\vec{r})$ a complicated function explicitly reported in [1], which accounts for near field effects. In fact, it is important to realize that the first optical element of the optical beamline will be placed at about 300 m from the end of the straight section. Such distance is comparable with the straight section length. Thus, one needs to know how edge radiation propagates in the near zone in order to characterize the pulse at the position of the optical element.

Since we deal with radiation from a filament beam with a given longitudinal profile, we should multiply the single-electron result by the squared-modulus of the Fourier transform of the temporal profile of the bunch, $\bar{f}(\omega)$. Moreover, in order to calculate the spatial density distribution of the number of photons per pulse we should integrate this product in $d\omega$. Being interested in coherent emission around the modulation wavelength, we can consider the wavelength in $dW/(d\omega dS)$ fixed. This amounts to a multiplication by $\int_0^\infty d\omega \left|\bar{f}(\omega)\right|^2 = \sqrt{\pi}N^2a_f^2/(4\sigma_T)$, where N is the number of electrons in the bunch, leading to

$$\frac{dN_{ph}}{dS} = \frac{\sqrt{\pi}}{16\pi^2}\frac{N^2\alpha a_f^2}{cL\sigma_T}F(z,\vec{r}) \ , \qquad (2)$$

where $\alpha \equiv e^2/(\hbar c) = 1/137$ is the fine structure constant.

We considered the case for $|a_f| = 0.1$, $L = 200$m, $\sigma_T \simeq 80$ fs and $N \simeq 6 \cdot 10^9$ (i.e. about 1 nC). Since the first element of the optical beamline is foreseen to be placed at about 300 m from the separating magnet (see Fig. 2), and since we measure z from the center of the straight section, we set our observation plane at $z = 400$ m. We used Eq. (2) to calculate the photon density distribution. We cross-checked our analytical results with the code SRW. Horizontal and vertical cuts along the contour plot for the photon density distribution are compared with Eq. (2) in Fig. 5. Contrarily to the x-ray pulse, which is peaked on-axis, the edge-radiation pulse is peaked in the forward direction at an angle of a few tens of microradians. The diameter of the spatial distribution of edge radiation at the first optical element will be about 3 cm, which fits with the aperture of the photon beamline. The total number of photons between the first two minima of the distribution function (at $r = 0$ cm and $r \simeq 2.2$ cm respectively) is obtained integrating in dS. For parameters selected above, $N_{ph} \simeq 2 \cdot 10^{12}$ photons.

The optical pulse is naturally synchronized with the XFEL pulse. Thus, once edge-radiation is transported to the experimental area, single-shot cross-correlation with the pump-laser pulse can be performed, yielding the time delay between the pump-laser and the XFEL pulse.

In conclusion, our analysis demonstrates the feasibility of pump-probe experiments at XFELs with femtosecond temporal resolution, based on timing of XFEL pulses to optical pulses from an external pump-laser. Technical realization will be rather simple and cost-effective since it is essentially based on technical components (optical-replica synthesizer) being already included in the design of the European XFEL.

REFERENCES

[1] G. Geloni, E. Saldin, E. Schnedimiller and M. Yurkov, Opt. Comm. 281, 37623770 (2008)